

# A note on complexity=anything conjecture in AdS Gauss-Bonnet gravity

---

Xuanhua Wang,<sup>a,\*</sup> Ran Li,<sup>b,\*</sup> Jin Wang<sup>c,d,\*</sup>

<sup>a</sup>Center for Theoretical Interdisciplinary Sciences, Wenzhou Institute, University of Chinese Academy of Sciences, Wenzhou, Zhejiang 325001, China

<sup>b</sup>School of Physics, Henan Normal University, Xinxiang, Henan 453007, China

<sup>c</sup>Department of Chemistry, Stony Brook University, Stony Brook, NY 11794, USA

<sup>d</sup>Department of Physics and Astronomy, Stony Brook University, Stony Brook, NY 11794, USA

E-mail: [wangxh@ucas.ac.cn](mailto:wangxh@ucas.ac.cn), [liran@htu.edu.cn](mailto:liran@htu.edu.cn), [jin.wang.1@stonybrook.edu](mailto:jin.wang.1@stonybrook.edu)

**ABSTRACT:** It has been suggested that quantum complexity is dual to the volume of the extremal surface, the action of the Wheeler-DeWitt patch, and the spacetime volume of the patch. Recently, it was proposed that a generalized volume-complexity observable can be formulated as an equivalently good candidate for the dual holographic complexity. This proposal is abbreviated as “complexity=anything”. This proposal offers greater flexibility in selecting extremal surfaces and evaluating physical quantities (e.g., volume or action) on these surfaces. In this study, we explore the complexity=anything proposal for Gauss-Bonnet black holes in asymptotic anti-de Sitter space in various dimensions. We demonstrate that this proposal guarantees the linear growth of the generalized volume at late time regardless of the coupling parameters for four-dimensional Gauss-Bonnet gravity. However, this universality is not upheld for higher dimensions. Besides, discontinuous deformations of the extremal surfaces emerge when multiple peaks exist in the effective potential, which is a reminiscence of a phase transition. In addition, we provide the constraints on the coupling parameter of the five dimensional models to quantify the generalized volume as a viable candidate for holographic complexity.

---

\*Corresponding authors

---

## Contents

<b>1</b>	<b>Introduction</b>	<b>1</b>
<b>2</b>	<b>Gauss-Bonnet-AdS black holes</b>	<b>3</b>
<b>3</b>	<b>CAny</b>	<b>4</b>
<b>4</b>	<b>Codimension-one extremal slices for Gauss-Bonnet in 4D</b>	<b>6</b>
4.1	Existence of local maxima	6
4.2	Dipping and non-Dipping branches	8
4.3	Phase transition of the extremal slice	9
<b>5</b>	<b>Codimension-one extremal slices for Gauss-Bonnet in 5D</b>	<b>11</b>
5.1	Existence of local maxima	11
5.2	Couplings outside the allowed range	13
<b>6</b>	<b>Conclusion</b>	<b>15</b>

---

## 1 Introduction

The holography of black holes has triggered much excitement and progress in our understanding of black holes over the last decade. At the core of this treatment lies the central dogma that black holes can be treated as standard quantum systems, exhibiting unitary evolution [1]. It is known that the entanglement entropy of a black hole is encoded in the area of its horizon after the Page time [2, 3]. While the entropy of a black hole increases only for a finite duration before thermalization, the volume of its interior and the length of the wormhole for a two-sided AdS black hole continue to increase [4]. Consequently, it has been suggested that a new quantum information measure is needed to capture the growth of the wormhole. Various concepts have emerged in this endeavor, linking volumes to the complexities of decoding information within the black hole, and several explicit calculations have been developed to demonstrate this duality [5–21].

Quantum complexity is a measure of least steps to complete a task by applying gates only from a set of finite simple operations. The ambiguity in the exact value of complexity comes from the arbitrariness of the choice of gate set and the cost assigned to each gate. It was argued that rather than a shortcoming, this ambiguity connects nicely with the ambiguity of rescaling freedom of the length/volume in its holographic dual [8, 9]. The scaling of the complexity with the size of the problem is the robust property and the quantum circuit complexity is shown to grow linearly with the number of Haar-random two-qubit quantum gates [22].

Inspired by the ER=EPR proposal [23], the observation of linear growth of the worm-hole length and the switchback effect of external perturbations, it was proposed that the quantum complexity is dual to volume of the codimension-one maximal slice (Complexity-Volume proposal, or CV) [5, 6], gravitational action in the Wheeler-DeWitt patch (Complexity-Action proposal, or CA) [24–29] and the spacetime volume of the Wheeler-DeWitt patch (Complexity-Volume proposal 2.0, or CV2.0) [7]. In the CV conjecture, the holographic complexity is dual to the maximal volume of the hypersurface anchored at the boundary CFT slice  $\Sigma_{\text{CFT}}$ , viz.

$$C_V(\Sigma_{\text{CFT}}) = \max_{\partial\mathcal{B}=\Sigma_{\text{CFT}}} \left[ \frac{\mathcal{V}(\mathcal{B})}{G_N \ell_{\text{bulk}}} \right], \quad (1.1)$$

where  $\mathcal{B}$  is the bulk hypersurface. While the CA conjecture states that the complexity is represented by the integral of the gravitational action in the Wheeler-DeWitt patch, which is the domain of dependence of the slice  $\mathcal{B}$ , i.e.

$$C_A(\Sigma_{\text{CFT}}) = \frac{I_{\text{WDW}}}{\pi \hbar}. \quad (1.2)$$

The CV2.0 proposal combines the CV and CA conjectures and proposes that the complexity is simply given by the spacetime volume of the Wheeler-DeWitt patch anchored at the given boundary states,

$$C_{V2}(\Sigma_{\text{CFT}}) = \frac{V_{\text{WDW}}}{G_N \ell_{\text{bulk}}^2}. \quad (1.3)$$

Recently, it was realized that such dual of holographic complexity that follows the linear growth and switchback effect at late times can be extended to an infinite family of observables of either codimension zero or one [8, 9, 30]. For codimension-one observables, which is the focus of this paper, the generalized volume is given by

$$C_{\text{gen}}(\tau) = \max_{\partial\Sigma(\tau)=\Sigma_{\text{CFT}}} \left( \frac{1}{G_N L} \int_{\Sigma(F_2)} d^{D-1} \sigma \sqrt{\hbar} F_1(g_{\mu\nu}; X^\mu(\sigma)) \right), \quad (1.4)$$

where the slice  $\Sigma(F_2)$  is the extremal surface for a scalar function  $F_2$  and  $\tau$  is the boundary time. Notably,  $F_2$  can be any scalar function and is not necessarily the same as  $F_1$  in the integrand. It is shown that at the late times, different choices of the functions  $F_2$  result in the same late-time behavior for the generalized volume [8]. Therefore, demonstrating the simpler case  $F_1 = F_2$  should suffice for the discussion. The proposal of Complexity=Anything (CAny) is useful in probing the singularities of black holes by tuning the coupling parameters [9, 30]. Recent development extends the CAny to de-Sitter spaces [31] and RN-AdS black holes [10]. The details of this proposal will be delineated in the subsequent sections.

The goal of this paper is to explore the generalized CAny proposal of the codimension-one surfaces for Gauss-Bonnet black holes in four dimensions and higher. We show that in four dimension the effective potentials for the Gauss-Bonnet black holes, which dictate the time evolution of the extremal surfaces, are qualitatively different from those in higher

dimensions due to the existence of multiple horizons. This feature in 4D Gauss-Bonnet black holes guarantees the linear growth of the generalized volume at late time regardless of the coupling parameters chosen. This trait of universal linear growth is absent for the Gauss-Bonnet black hole of higher dimensions. In addition, we explore the scenario when multiple extremal surfaces exist and show that different rates of volume growth can be assigned to the surfaces. We demonstrate the time evolution of conserved momenta corresponding to different configurations of the extremal surfaces and illustrate the conditions for the generalized volume to be qualified as the dual of the holographic complexity. In Sec. 2, we give the background for the essential features of Gauss-Bonnet black holes. In Sec. 3, we review the CAny proposal and demonstrate how it works for codimension-one observables. Sec. 4 is concentrated on investigating in depth the CAny proposal in 4D Gauss-Bonnet gravity and the analysis of 5D Gauss-Bonnet gravity is provided in Sec. 5. We conclude our discussion in the last section.

## 2 Gauss-Bonnet-AdS black holes

The Gauss-Bonnet Lagrangian is a natural generalization of general relativity which modifies the equations of motion in dimensions larger than four. In 4D, the Gauss-Bonnet term is topological and does not contribute to the equations. Various techniques have been constructed to obtain a consistent nontrivial 4D Gauss-Bonnet gravity and the related issues have triggered vehement discussions. The recent development and the related issues are reviewed in Ref. [32]. Though issues in 4D are more subtle and not completely understood, it is still worthwhile to explore the full consequences of the theory.

Gauss-Bonnet-AdS black holes in 4D has two horizons which means that the central singularity is time-like [33–35]. In  $D \geq 5$ , the solution only has one horizon like the Schwarzschild solution. The topology of Gauss-Bonnet black holes is an active research topic and has been investigated in Refs. [36–40]. The action for the GB-AdS black hole is given by [41]

$$\mathcal{S} = \frac{1}{16\pi} \int d^D x \sqrt{-g} (R - 2\Lambda + \tilde{\alpha} \mathcal{L}_{GB}), \quad (2.1)$$

where  $\mathcal{L}_{GB} = R^2 - 4R_{\mu\nu}R^{\mu\nu} + R_{\mu\nu\rho\sigma}R^{\mu\nu\rho\sigma}$  and  $\Lambda = -\frac{(D-1)(D-2)}{2L^2}$ . For simplicity, we denote  $\alpha = \tilde{\alpha}(D-3)(D-4)$ . Note that the GB coupling  $\tilde{\alpha}$  is scaled as  $\frac{1}{D-4}$  which cancels out the  $(D-4)$  factor in the definition of  $\alpha$ . Taking the limit  $D \rightarrow 4$  results in the effective equation of the Einstein-Gauss-Bonnet-AdS model in 4D. The causality bound from the boundary CFT requires  $|\alpha/L^2| \ll 1$  [42]. On the other hand, a well-defined vacuum of the theory also requires that  $0 \leq \frac{4\alpha}{L^2} \leq 1$ . For spherically symmetric solution, the metric is given by

$$ds^2 = -f(r)dt^2 + f(r)^{-1}dr^2 + r^2 d\Omega_{D-2}^2, \quad (2.2)$$

$$(2.3)$$

where  $\Omega_{D-2}$  is the phase-space volume of the  $(D-2)$ -dimensional sphere. In Eddington-Finkelstein coordinates, it reads

$$ds^2 = -f(r)dv^2 + 2dvdr + r^2 d\Omega_{D-2}^2, \quad (2.4)$$

where the infalling coordinate  $v = t + r_*(r)$  with  $r_*(r) = -\int_r^\infty \frac{dr'}{f(r')}$ , and the lapse function  $f(r)$  is given by

$$f(r) = 1 + \frac{r^2}{2\alpha} \left[ 1 - \sqrt{1 + 4\alpha \left( \frac{w}{r^{D-1}} - \frac{1}{L^2} \right)} \right]. \quad (2.5)$$

Here,  $w = 16\pi GM / ((D-2)\Omega_{D-2})$  is the re-scaled mass of the black hole. The location of the horizon satisfies  $f(r_h) = 0$ , viz.,

$$w = r_h^{D-3} \left( 1 + \frac{r_h^2}{L^2} + \frac{\alpha}{r_h^2} \right). \quad (2.6)$$

The temperature of the black hole is given by

$$T_{BH} = \frac{f(r)'}{4\pi} \Big|_{r=r_h} = \frac{(D-3)r_h^2 + (D-1)r_h^4/L^2 + (D-5)\alpha}{4\pi r_h (r_h^2 + 2\alpha)}. \quad (2.7)$$

### 3 CAny

For the codimension-one observable, CAny generalizes the CV and the CA proposals to observables of the form

$$C_{gen}(\tau) = \max_{\partial\Sigma(\tau)=\Sigma_{CFT}} \left( \frac{1}{G_N L} \int_{\Sigma} d^{D-1}\sigma \sqrt{h} F_1(g_{\mu\nu}; X^\mu(\sigma)) \right), \quad (3.1)$$

where the slice  $\Sigma$  is the extremal surface for the scalar function  $F_2$  which is not necessarily the same as the scalar function  $F_1$  in the integrand and  $\tau$  is the boundary CFT time with  $\tau = 2t_L = 2t_R$ . The codimension-one extremal slice can be easily generalized to codimension-zero case where the integration is over the spacetime region enclosed by two extremal slices plus the contribution from the two codimension-one slices. It was argued that such observables grow linearly with time at late times and exhibit the switchback effect. In this study, we investigate the CAny conjecture in the Gauss-Bonnet gravities and discuss the condition for such conjecture to hold.

For simplicity, we pick  $F_1 = F_2$  and consider the spherically symmetric scalar functions. Choosing the parameterization  $(v(\sigma), r(\sigma), \vec{\Omega})$ , we have

$$C_{gen}(\tau) = \frac{\Omega_{D-2}}{G_N L} \int_{\Sigma} d\sigma \sqrt{-f(r)\dot{v}^2 + 2\dot{v}\dot{r}} F_1(r). \quad (3.2)$$

Note that by choosing  $F_1 = 1$ , it returns to the CV proposal. One can identify the generalized complexity as the action and the integrand as the Lagrangian. From the classical equation of motion  $\frac{\partial S}{\partial q^i} = \frac{\partial L}{\partial \dot{q}^i} \Big|_{\partial\Sigma}$ , we obtain

$$\frac{dC_{gen}}{d\tau} = \frac{1}{2} \frac{\partial(\sqrt{h}F_1)}{\partial \dot{t}} \Big|_{\partial\Sigma(\tau)} = \frac{1}{2} P_t \Big|_{\partial\Sigma(\tau)}. \quad (3.3)$$

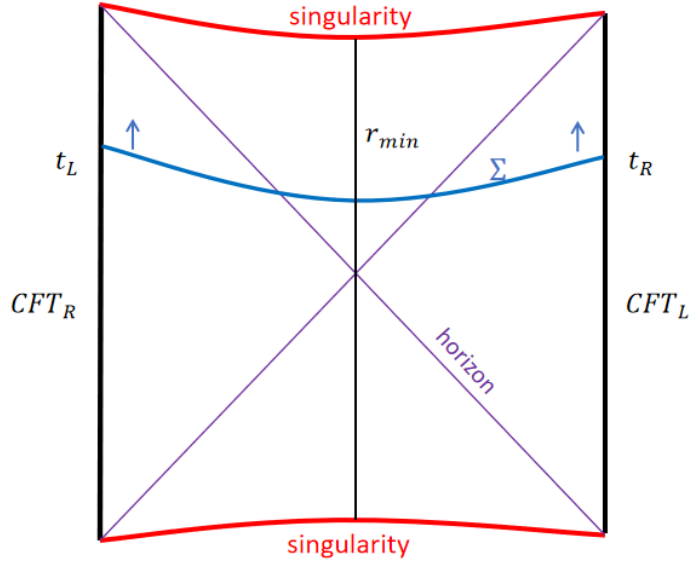


**Figure 1.** Extremal slices

The generalized complexity is diffeomorphism invariant and we employ our freedom of reparametrization to pick the gauge condition

$$\sqrt{-f(r)\dot{v}^2 + 2\dot{v}\dot{r}} = F_1(r) \left(\frac{r}{L}\right)^{D-2}. \quad (3.4)$$

The momentum  $P_\nu$  conjugate to the infalling time  $\nu$  is

$$P_\nu = \frac{\partial \mathcal{L}}{\partial \dot{\nu}} = \dot{r} - f(r)\dot{\nu}, \quad (3.5)$$

where the dots are the derivatives taken with respect to the parameter  $\sigma$  which increases from the left AdS boundary to the right AdS boundary. The above two equations give the extremality conditions:

$$\dot{r} = \pm \sqrt{P_\nu^2 + f(r)F_1^2 \left(\frac{r}{L}\right)^{2(D-2)}}, \quad (3.6)$$

$$\dot{\nu} = \frac{1}{f(r)} \left( -P_\nu \pm \sqrt{P_\nu^2 + f(r)F_1^2 \left(\frac{r}{L}\right)^{2(D-2)}} \right) = \frac{1}{f(r)} (-P_\nu + \dot{r}). \quad (3.7)$$

Comparing the equations with the motion of a classical particle, we obtain the equations of motion

$$\dot{r}^2 + \tilde{U}(r) = P_\nu^2 \quad \text{with} \quad \tilde{U}(r) = -f(r)F_1(r)^2 \left(\frac{r}{L}\right)^{2(D-2)}. \quad (3.8)$$

Note that

$$\dot{\nu} = \dot{t} + \frac{dr_*}{dr} \frac{dr}{d\sigma} = \dot{t} + \frac{\dot{r}}{f(r)}, \quad (3.9)$$

and the conjugate momentum  $P_\nu$  is conserved for a specific boundary time  $\tau$ . Combining it with the above extremality condition Eq. (3.7), we have

$$\dot{t} = -\frac{P_\nu}{f(r)}. \quad (3.10)$$

From the equations for  $\dot{t}$ ,  $\tilde{U}(r)$ , we can recast the generalized volume as

$$C_{gen}(\tau) = \frac{\Omega_{D-2}}{G_N L} \int_\Sigma^\tau dt \frac{\tilde{U}(r(t))}{P_\nu}. \quad (3.11)$$

One needs to be careful that here the integration is taken on the extremal surface so that  $P_\nu$  in the denominator is a constant. The boundary time  $\tau$  is related to the conjugate momentum by

$$t = \tau/2 = - \int_{r_{\min}}^\infty dr \frac{P_\nu}{f(r) \sqrt{P_\nu^2 - \tilde{U}(r)}}, \quad (3.12)$$

where  $r_{\min}$  is the minimal radius lying on the timelike surface  $t = 0$ . The growth rate of the complexity

$$\frac{dC_{gen}}{d\tau} = \frac{\Omega_{D-2}}{G_N L} P_\nu(\tau) \quad (3.13)$$

can be calculated from the effective potential. The linear growth of  $C_{gen}$  at late times is dedicated by the condition that  $\lim_{\tau \rightarrow \infty} P_\nu(\tau) := P_\infty$  is constant and the effective potential  $\tilde{U}(r)$  has a local maximum inside the horizon. In this case,

$$\lim_{\tau \rightarrow \infty} \frac{dC_{gen}}{d\tau} = \frac{\Omega_{D-2}}{G_N L} P_\infty = \frac{\Omega_{D-2}}{G_N L} \sqrt{\tilde{U}(r_f)}, \quad (3.14)$$

where  $r = r_f$  is the radius of the local maximum. In certain parameter regimes, the effective potential may have more than one local maxima as shown in Fig. 2.

## 4 Codimension-one extremal slices for Gauss-Bonnet in 4D

### 4.1 Existence of local maxima

For Gauss-Bonnet black hole, one simplest extension beyond the CV proposal in CAny is to add a higher curvature terms such as the square of Weyl tensors

$$C^2 = \frac{2}{D(D-1)} R^2 - \frac{4}{D-1} R_{\mu\nu} R^{\mu\nu} + R_{\mu\nu\rho\sigma} R^{\mu\nu\rho\sigma}. \quad (4.1)$$

The analysis is much simplified in 4D due to the different topology of Gauss-Bonnet-AdS black holes in 4D. For the spherically symmetric solutions of Gauss-Bonnet black holes in 4D, the square of Weyl tensor is

$$C^2(r) = \frac{12L^2 w^2 (L^2 (r^3 + \alpha w) - 4\alpha r^3)^2}{(L^2 (r^4 + 4\alpha r w) - 4\alpha r^4)^3}. \quad (4.2)$$

One straightforward generalization of the CV proposal (which is recovered by setting  $F_1 = 1$ ) is to pick  $F_1(r) = 1 + \lambda L^4 C^2(r)$ . This scalar function is the simplest nontrivial function in Einstein gravity in vacuum and is the most studied one. We choose this function so that it is easier to compare with existing studies.<sup>1</sup> Then, the generalized holographic complexity is defined as the integration of the scalar function on the space volume that extremizes the integral, viz.,

$$C_{gen}(\tau) = \frac{\Omega_{D-2}}{G_N L} \int_{\Sigma} d\sigma \sqrt{-f(r)\dot{v}^2 + 2\dot{v}\dot{r}} (1 + \tilde{\lambda} L^4 C^2(r)). \quad (4.3)$$

To ensure that the late time evolution of the generalized complexity increases linearly with the boundary time  $\tau$ , we plot the effective potential  $\tilde{U}(r)$  as a function of radius  $r$ . For a reminder, the effective potential reads,

$$\tilde{U}(r) = -f(r)F_1(r)^2 \left(\frac{r}{L}\right)^{2(D-2)} = -f(r) (1 + \lambda L^4 C^2(r))^2 \left(\frac{r}{L}\right)^{2(D-2)}. \quad (4.4)$$

For the Gauss-Bonnet-AdS black hole in 4D, its Penrose diagram is similar to that of a charged black hole with two horizons. For spacetime regions inside the inner horizon or outside the outer horizon, i.e.,  $r < r_-$  or  $r > r_+$ , the lapse function is positive  $f(r) > 0$ . For spacetime regions between the two horizons,  $f(r) < 0$ . Therefore, the effective potential  $\tilde{U}(r)$  is positive between the horizons and negative otherwise as shown in Fig. 2. This ensures that the effective potential always has the local maximum  $\tilde{U}(r_f)$  inside the horizon, which is the condition for the linear growth of complexity at late times. We will further delineated this point later.

To see that any such observables in  $D = 4$  suffice as candidates for holographic complexity, we show that  $\lim_{\tau \rightarrow \infty} P_{\nu}(\tau) = P_{\infty}$  is constant. Recall that the boundary time is

$$\tau = -2 \int_{r_{min}}^{\infty} dr \frac{P_{\nu}}{f(r) \sqrt{P_{\nu}^2 - \tilde{U}(r)}}, \quad (4.5)$$

where  $r_{min}$  is determined by  $P_{\nu}^2 - \tilde{U}(r_{min}) = 0$ . The lapse function  $f(r)$  is continuous and nonzero between the two horizons. For  $P_{\nu}^2 < \tilde{U}(r_f)$  where  $r_f$  is the radius of the local maximum of the effective potential,  $\tilde{U}(r) \simeq P_{\nu}^2 + \tilde{U}'(r_{min})(r - r_{min})$  near  $r = r_{min}$ . The integrand  $\frac{P_{\nu}}{f(r) \sqrt{P_{\nu}^2 - \tilde{U}(r)}}$  of Eq. (4.5) is regular everywhere except at  $r = r_{min}$ . Notice that for  $U'(r_{min}) \neq 0$ , one can take the Cauchy principal value and the integral which gives the boundary time  $\tau$  is finite. At late times,  $\tau \rightarrow \infty$  and it corresponds to  $P_{\nu}^2 \rightarrow \tilde{U}(r_f)$ . In this case,  $\tilde{U}(r) \simeq P_{\nu}^2 + \frac{1}{2} \tilde{U}''(r_f)(r - r_f)^2 + O(r - r_f)^3$  near  $r = r_f$ . It is easy to see that as long as  $r = r_f$  is the local maximum for  $\tilde{U}(r)$ , the function in the integrand is no longer integrable in the domain. In other words, the integral is divergent with the irregular point at  $r = r_f$ . This suggests that when  $P_{\nu}$  approaches  $\tilde{U}(r_f)$ , the result of the integral which gives  $\tau$  can take arbitrarily large values. Therefore, at late times  $\tau \rightarrow \infty$ , the conjugate

---

<sup>1</sup>The simpler choices of scalar functions such as  $R^2$  and  $R_{\mu\nu}R^{\mu\nu}$  do not contribute in the vacuum solutions of the Einstein gravity, therefore are not of particular interest in related studies.



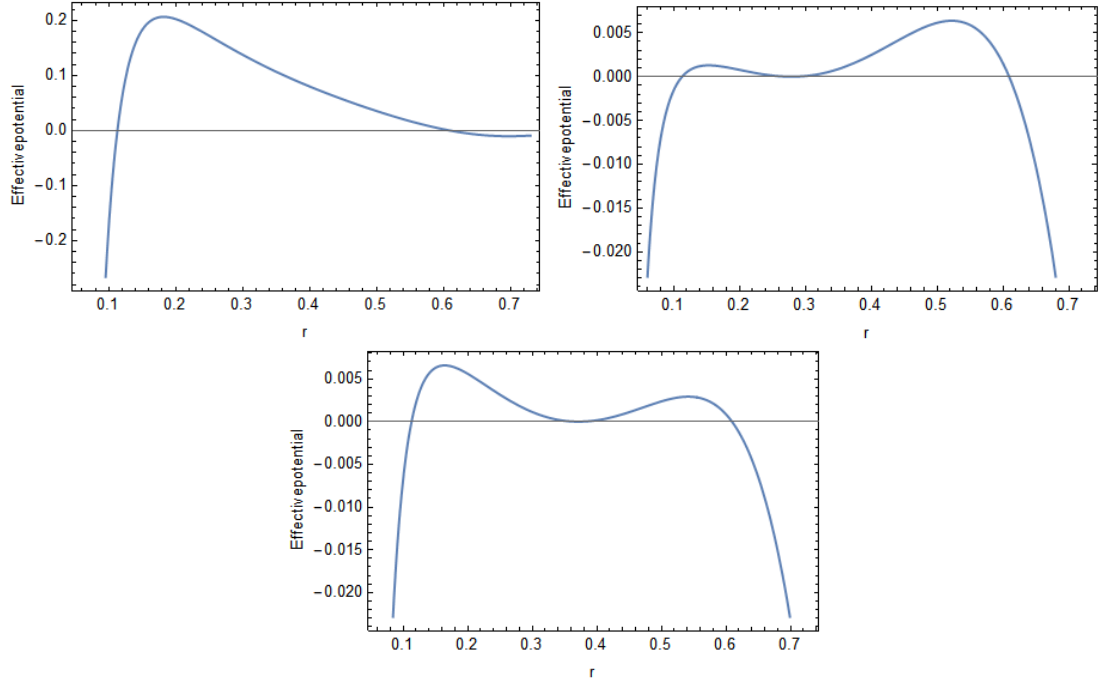


**Figure 2.** Effective potential  $\tilde{U}(r)$  as a function of radius  $r$  in 4D. Left:  $\lambda = -0.1$ . Right:  $\lambda = -0.01$ . Bottom:  $\lambda = -0.02$ .  $\tilde{U}(r)$  vanishes on the inner and outer horizons and stays positive between them. This feature of the effective potential is universal in 4D Gauss-Bonnet black holes. For all,  $L = w = 1$ ,  $\alpha = 0.1$ .

momentum  $P_\nu$  approaches a constant  $P_\nu^2 \rightarrow \tilde{U}(r_f)$ , and the growth rate of the complexity is

$$\lim_{\tau \rightarrow \infty} \frac{dC_{gen}}{d\tau} = \frac{\Omega_{D-2}}{G_N L} \sqrt{\tilde{U}(r_f)}. \quad (4.6)$$

Therefore, Any proposal has the natural realization at  $D = 4$  in Gauss-Bonnet-AdS black holes. No additional constraints or regularization for the scalar field is required.

## 4.2 Dipping and non-Dipping branches

In the case of 4D Gauss-Bonnet-AdS black holes, the extremal surface can not approach arbitrarily close to the singularity for arbitrarily large conjugate momenta as it does for planar black holes in Einstein’s theory [9]. The effective potentials in Ref. [9] diverge to infinity as  $r \rightarrow 0$ , and the equation  $P_\nu^2 = \tilde{U}$  always has a solution for arbitrarily large conjugate momentum  $P_\nu$ . On the other hand, the effective potential for a 4D Gauss-Bonnet-AdS black hole [see Fig. 2] is similar to that of RN-AdS black holes, where the effective potential approaches negative infinity as  $r \rightarrow 0$  [10]. The “dipping branch” in this scenario corresponds to the time evolution of  $P_\nu$  approaching  $P_\infty$  from above, i.e.,  $P_\nu$  decreases with the boundary time  $\tau$  which is given by

$$\tau = -2 \int_{r_{\min}}^{r_{\max}} dr \frac{P_\nu}{f(r) \sqrt{P_\nu^2 - \tilde{U}(r)}}, \quad (4.7)$$

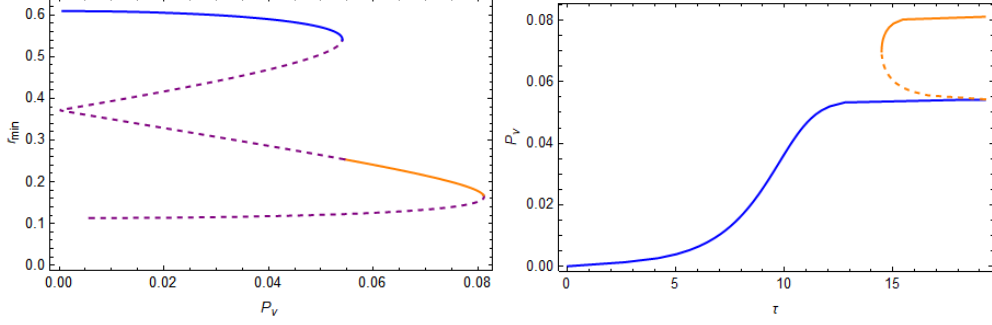


**Figure 3.** Conserved momentum when effective potential has two local maxima with global maximum locates inside. Left: the minimal radius  $r_{\min}$  of the extremal surface vs conserved momentum at  $\lambda = -0.02$ . The dashed curves correspond to the hypersurfaces that do not have boundaries at  $\Sigma_{\text{CFT}}$ . Right: boundary time vs conserved momentum at  $\lambda = -0.02$ . The dashed lines correspond to the hypersurface that has decreasing  $P_\nu$  and increasing  $r_{\min}$  as time evolves. The generalized volume evaluated on this slice is smaller than its counterpart measured along the blue curve. For both,  $L = w = 1$ ,  $\alpha = 0.1$ .

where  $r_{\min}$  the solution of  $P_\nu = \tilde{U}(r)$ . This process is represented by the orange solid lines in Fig. 3 (a) going from right to left and also by the dashed orange branch in Fig. 3 (b). One can compute numerically that the transitioning point from no dipping branch to the emergence of a dipping branch occurs at  $\lambda \simeq -0.05$ . It is worthwhile to point out that the extremal surfaces corresponding to the dipping branches in both the 4D Gauss-Bonnet gravity and the planar Einstein gravity do not yield the maximal holographic complexity at late times. This can be seen by comparing the late-time generalized volume evaluated on the dipping branch with that on the non-dipping branch

$$\lim_{\tau \rightarrow \infty} (C_{\text{no-dip}}(\tau) - C_{\text{dip}}(\tau)) = \lim_{\tau \rightarrow \infty} \frac{\Omega_{D-2}}{G_N L} \int_{t=0}^{t=\tau} dt \left( P_\infty - \frac{\tilde{U}(r(t))}{P_\infty} \right). \quad (4.8)$$

At late times,  $P_\nu(\tau) \rightarrow P_\infty$  and the  $\tilde{U}(r(t)) \leq P_\infty^2$ , therefore, the RHS of the above equation is positive. Therefore, we can draw the following conclusion: *the surface yielding the maximal complexity is always the one whose minimal radius approaches the local maximum of the effective potential.*

### 4.3 Phase transition of the extremal slice

One feature of the holographic complexity in 4D Gauss-Bonnet-AdS black holes is the appearance of multiple local maxima in the effective potential as illustrated in Fig. 2 (b) and (c). Consequently, the late-time behavior of the generalized volume is now characterized by two different branches, resulting in different rates of increase for the generalized volume-complexity.

Notably, there is no continuous variation from one branch to the other along the trajectory of equations of motion. The time evolution of the conserved momentum  $P_\nu$  with respect to the boundary time  $\tau$  extends to an infinite future, ultimately approaching  $P_{\infty,R}$ , which is the asymptotic conserved momentum defined through Eq. (4.5) as  $\tau \rightarrow \infty$ . It is

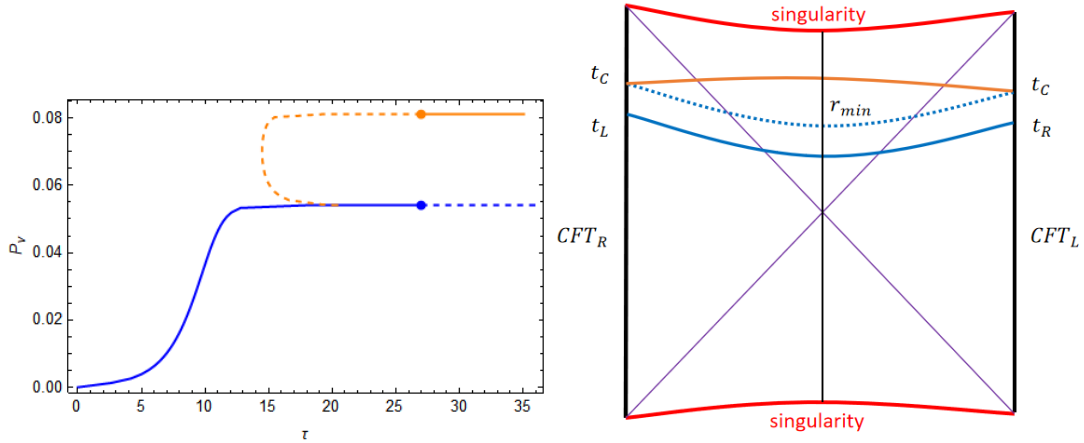


**Figure 4.** Coexistence of two branches of extremal surfaces at  $\lambda = -0.02$ . Left: the boundary time  $\tau$  vs the conserved momentum  $P_\nu$ . The two colors represent the two branches of the extremal surfaces. The blue curve represents the evolution from  $(0, 0)$ . The generalized volume-complexity along the blue curve, which is proportional to the area below the curves, is dominating at the beginning of coexistence of two branches. After some critical time  $t_C$ , the volume-complexity computed from the orange curve dominates, and the conserved momentum jumps to a higher value discontinuous. Right: the Penrose diagram of the process. For both,  $L = w = 1$ ,  $\alpha = 0.1$ .

the value of  $P_\nu$  at the right peak of the effective potential and is represented by the end value of the blue curve in Fig. 4 (a). Along the trajectory of equations of motion, the evolution of the generalized volume-complexity is determined either by the left or by the right local maximum of the effective potential. Both trajectories of  $P_\nu$  are smooth.

On the other hand, from the volume-complexity conjectures, the generalized volume-complexity  $C_{gen}$  is the maximum value evaluated on all the branches. This requirement results in discontinuous jumps of the extremal surface from the blue curve to the orange one closer to the singularity at time  $t_C$  as shown in Fig. 4. We remind that this “phase transition” is not describable by the equations of motion of the extremal surfaces (Eq. 3.7) but rather is from the definition of the volume-complexity

$$C_{gen} = \max_{\Sigma} \left( \frac{\Omega_{D-2}}{G_N L} \int_{\Sigma} P_\nu(\tau) d\tau \right), \quad (4.9)$$

where  $\Sigma$ ’s are the extremal surfaces.

In Fig. 4 (b), we demonstrate the two extremal surfaces in the Penrose diagram. At the critical time  $t_C$ , the volume-complexity evaluated on the two surfaces are the same. While post the critical-time, the surface closer to the singularity [the solid orange curve] has a larger volume-complexity. As shown in Fig. 3 (a), the non-dipping branch represented by the blue solid line on the top has a lower generalized volume at  $\tau \rightarrow \infty$ . The extremal surface that generates the largest volume complexity jumps to the one ending at the left peak of Fig. 2(c), and is represented by the orange solid line in Figs. 3 and 4. This behavior is a reminiscence of a phase transition and was briefly discussed in [10]. In particular, depending on the shape of the effective potential and in higher dimensional

cases, this phase transition between different branches of  $P_\nu - \tau$  diagrams can occur more than once. Overall, *the late-time behavior is always dictated by the maximal peak of the effective potential  $\tilde{U}(r)$  and the extremal surface after the transition always moves closer to the singularity.*

## 5 Codimension-one extremal slices for Gauss-Bonnet in 5D

In contrast to the four-dimensional case, Gauss-Bonnet black holes of dimensions higher than five exhibit the presence of only one horizon. For  $d > 4$ , the analysis is similar and easily generalized but it becomes more complicated due to Weyl tensor terms. Therefore, in this study, we will explicitly illustrate the five-dimensional case to demonstrate the constraints on the coupling parameter necessary for the existence of the extremal surface at late times.

### 5.1 Existence of local maxima

In 5D, the black hole has a minimal black hole mass condition  $w > \alpha$ . It has a single horizon and its corresponding effective potential does not automatically admit a local maximum inside the horizon as in the case of 4D. Notably, the lapse function  $f(r) < 0$  for the inside of the black hole  $r < r_h$ , which leads to the effective potential being positive inside the horizon, i.e.,  $\tilde{U}(r) > 0$ . Since  $\tilde{U}(r) < 0$  for  $r > r_h$ , it does not automatically ensure the existence of the local maximum as that in 4D. Therefore, the volume-complexity does not have the same simple universality as in 4D.

For the spherically symmetric solutions of Gauss-Bonnet black holes in 5D, the square of Weyl tensor is

$$C^2(r) = \frac{8L^2w^2 (L^2 (3r^4 + 4\alpha w) - 12\alpha r^4)^2}{r^4 (L^2 (r^4 + 4\alpha w) - 4\alpha r^4)^3} \quad (5.1)$$

The effective potential reads

$$\tilde{U}(r) = -f(r) \left( 1 + \lambda \frac{8L^6w^2 (L^2 (3r^4 + 4\alpha w) - 12\alpha r^4)^2}{r^4 (L^2 (r^4 + 4\alpha w) - 4\alpha r^4)^3} \right)^2 \left( \frac{r}{L} \right)^6. \quad (5.2)$$

In this case, it is difficult to directly solve for the local maximum of  $\tilde{U}(r)$ . Nevertheless, one may notice that the effective potential  $\tilde{U}(r) \rightarrow \infty$  as  $r \rightarrow 0$  as illustrated in Fig. 5. The future null slice which hugs the singularity will always be the global maximum when evaluating the integral. This point will be delineated in detail later.

For  $\lambda < 0$ , we now show that the extremal surface always exists if the coupling parameter  $\lambda$  lies within the range  $\lambda_c < \lambda < 0$  where  $\lambda_c$  is the critical coupling to be determined later. For  $\lambda < 0$ ,  $\lambda C^2(r) \rightarrow -\infty$  near the singularity. Since  $C^2(r) \rightarrow 0$  as  $r \rightarrow \infty$ , one can see that  $\tilde{U}(r)/f(r) = 0$  always has roots. For simplicity, we rewrite the square of Weyl tensor as

$$C^2(\mathcal{R}) \propto \frac{(3\mathcal{R} + \beta)^2}{\mathcal{R}(\mathcal{R} + \beta)^3}, \quad (5.3)$$

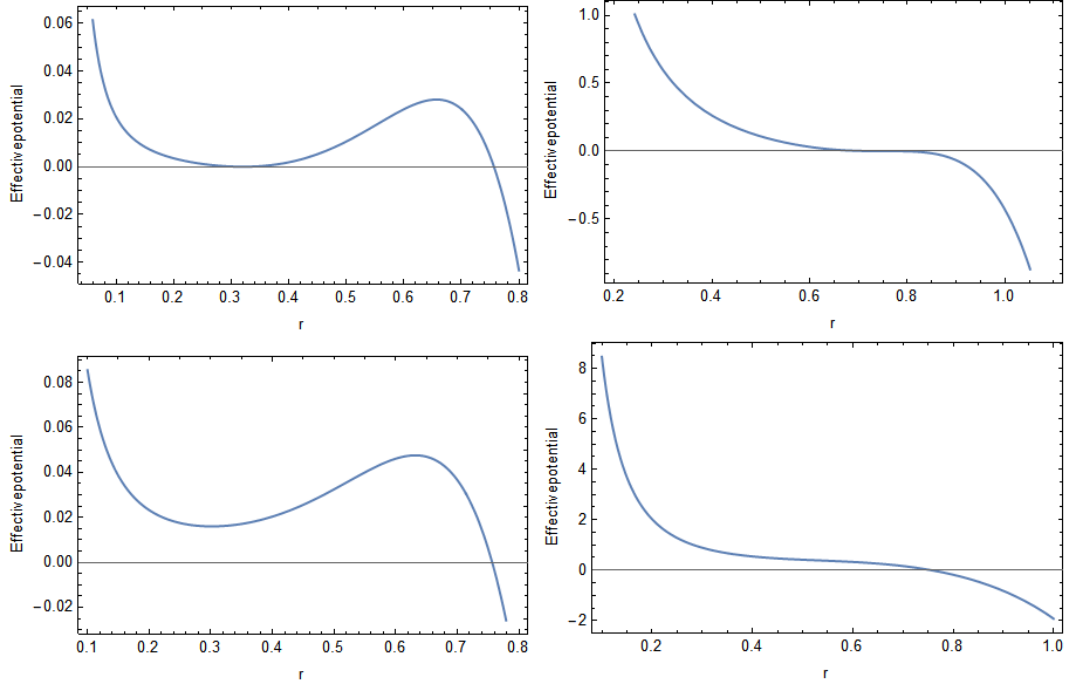


**Figure 5.** Effective potential  $\tilde{U}(r)$  as a function of radius  $r$  in 5D. (a)  $\lambda = -0.0005 > \lambda_c$ . This corresponds to the case that local maximum exists inside the horizon. (b)  $\lambda = -0.008877 = \lambda_c$ . This demonstrates the effective potential at exactly the critical point when the local maximum approaches the horizon and disappears. (c)  $\lambda = 0.001 < \lambda'_c$ . (d)  $\lambda = 0.01 > \lambda'_c$ . For all,  $L = w = 1$ ,  $\alpha = 0.1$ . Unlike the case in 4D,  $\tilde{U}(r) \rightarrow \infty$  close to the singularity  $r \rightarrow 0$ .

where  $\mathcal{R} = (L^2 - 4\alpha)r^4$  and  $\beta = 4\alpha w L^2$ . We remind that  $(L^2 - 4\alpha) > 0$  is required by the well-defined vacuum in the theory. One can check from the above formula Eq. (5.3) that  $dC^2(\mathcal{R})/d\mathcal{R} < 0$  holds for all  $\mathcal{R} > 0$ . Therefore, the equation for the effective potential

$$\tilde{U}(r) = -f(r)(1 + \lambda C^2(r))^2 (r/L)^{2(D-2)} = 0 \quad (5.4)$$

has roots inside the horizon when the coupling parameter satisfies  $\lambda_c < \lambda < 0$ , where  $\lambda_c$  is the critical value of  $\lambda$  that is determined by  $\lambda_c C^2(r_h) = -1$  where  $r_h$  is the radius of the horizon. The case  $\lambda = \lambda_c$  corresponds to when the local minimal of the effective potential is zero at the horizon. Obviously, for  $\lambda < \lambda_c$ , the effective potential  $\tilde{U}(r) > 0$  for  $r < r_h$  and it does not have a root inside the horizon. The effective potential  $\tilde{U}(r)$  monotonically decreases inside the horizon, therefore, in this case it does not have a local maximum. In conclusion, the above analysis proves that when  $\lambda_c < \lambda < 0$ , the requirement of linear growth for the observable  $C_{gen}$  at late times is satisfied. In addition, the analysis also holds for Gauss-Bonnet black holes of higher-dimensions.

For  $\lambda \geq 0$ , the effective potential satisfies  $\tilde{U}(r) > 0$  for  $r < r_h$  so that it does not have a root inside the horizon. We notice that the effective potential  $\tilde{U}(r) \propto -f(r)r^6(1 + \lambda C^2(r))^2$ .

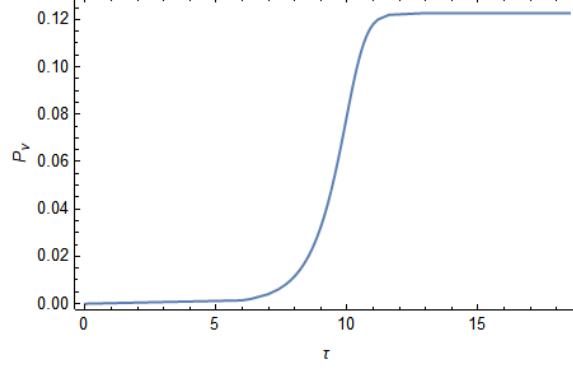


**Figure 6.** The change of conjugate momentum  $P_\nu$  with boundary time  $\tau$ .  $\lambda = -0.002$ ,  $L = w = 1$ , and  $\alpha = 0.1$ .

For  $r^2 \ll \alpha$  (near the singularity), one has

$$\begin{aligned} \frac{d(-f(r)r^6)}{dr^4} &= \frac{-2r^4 \left( \sqrt{-\frac{4\alpha}{L^2} + \frac{4\alpha w}{r^4} + 1} - 1 \right) - 3\alpha\sqrt{r^4} \sqrt{-\frac{4\alpha}{L^2} + \frac{4\alpha w}{r^4} + 1} + 6\alpha w - \frac{8\alpha r^4}{L^2}}{2\alpha\sqrt{-\frac{4\alpha}{L^2} + \frac{4\alpha w}{r^4} + 1}} \\ &\simeq \frac{3\alpha w - 3\alpha\sqrt{\alpha w}}{\alpha\sqrt{4\alpha w}} r^2 > 0. \end{aligned} \quad (5.5)$$

Both the effective potential and its derivative with respect to the radius  $r$  are positive inside the horizon and  $\tilde{U}(r_h) = 0$  on the horizon. This guarantees that when  $\lambda = 0$  there exists a local maximum  $\tilde{U}(r)$  inside the horizon. Since the square of Weyl tensor  $C^2(r)$  is a monotonically decaying function, it follows that there exists a maximal value of  $\lambda'_c \geq 0$  such that:

- (1) for  $0 \leq \lambda < \lambda'_c$ , the effective  $\tilde{U}(r)$  has a local maximum inside the horizon;
- (2) for  $\lambda > \lambda'_c$ ,  $d\tilde{U}(r)/dr < 0$  inside the horizon.

This completes the existence proof of the desired shape of the effective potential within a finite range of the coupling parameter. The maximal value  $\lambda'_c$  depends non-trivially on  $w, \alpha, L$  and can be determined numerically. The graphic illustration of the above results is shown in Fig. 5. Combining the analysis above, we conclude that  $C_{gen}$  is a well-behaved observable for the holographic complexity as long as  $\lambda_c < \lambda < \lambda'_c$  where  $\lambda_c = -1/C^2(r_h) < 0$  and  $\lambda'_c > 0$ .

As shown in Fig. 6, when the coupling parameter is within the above-mentioned range, the conserved momentum monotonically increases with time and approaches a finite asymptotic value  $P_\infty$ . In this case, the generalized volume-complexity has a constant rate of increase at late times as  $\lim_{\tau \rightarrow \infty} \frac{dC_{gen}}{d\tau} = \frac{\Omega_{D-2}}{G_N L} P_\infty$ .

## 5.2 Couplings outside the allowed range

In the preceding section, we showed the existence of the desired behaviors of the volume-complexity only for a finite range of coupling parameters. This is in contrast to the 4D case where no such constraints are necessary. On the other hand, even for the coupling

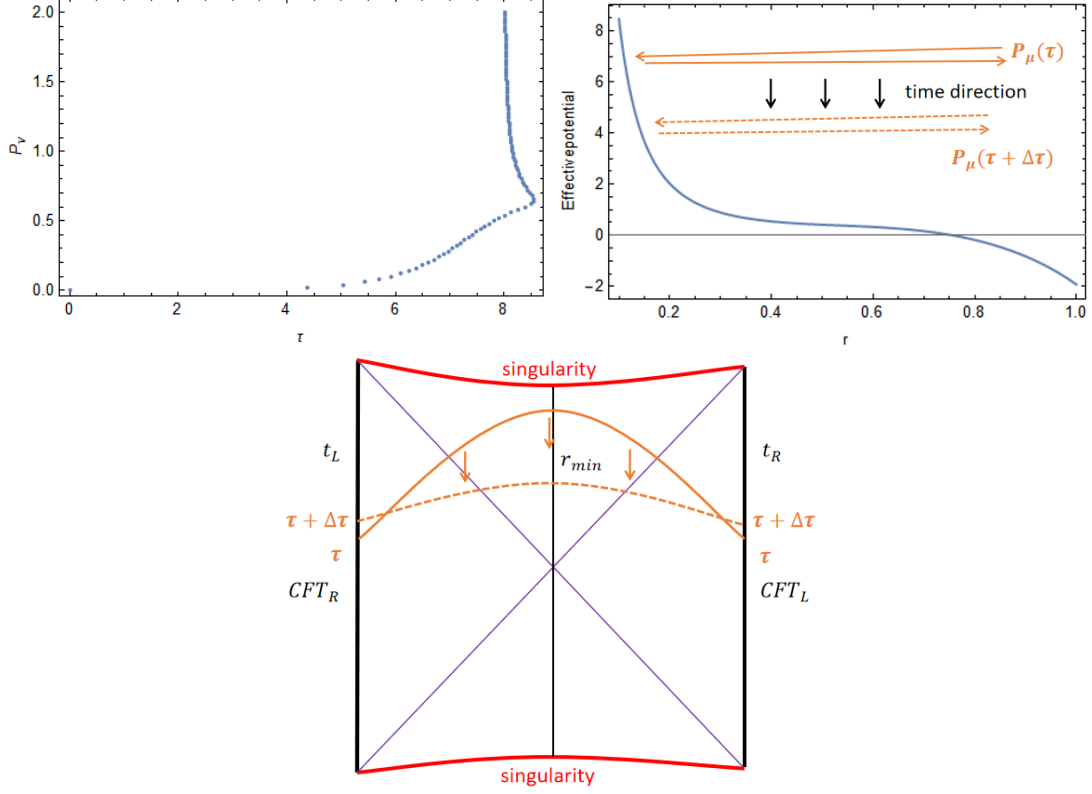


**Figure 7.** (a) Time evolution of the conserved momentum with  $\lambda = 0.01$ ,  $L = w = 1$ , and  $\alpha = 0.1$ . (b) Diagrammatic illustration of the evolution of the conserved momentum at large values in (a). (c) The Penrose diagram for the process in (b). The parameters are  $L = w = 1$ ,  $\alpha = 0.1$  and  $\lambda = -0.01$ .

parameters outside the desired range, we can just as well explore the behaviors of the conserved momentum and the extremal surfaces.

First of all, we can look at the evolution of the conserved momentum using Eq. (4.5). For example, for the coupling parameter  $\lambda = 0.01$  which is larger than the critical value  $\lambda'_c$ , the effective potential is monotonically decreasing as shown in Fig. 5 (d). We evolve the extremal surface from  $\tau = 0$  and  $P_\nu = 0$ . As shown in Fig. 7 (a), the evolution of the conserved momentum lasts only for a finite time before the extremal surface ceases to exist. On the other hand, if we start from an extremely large  $P_\nu$  which corresponds to the extremal surface extending arbitrarily close to the singularity,  $P_\nu$  rapidly decays to its final value and then no solutions exist any longer. This case is shown diagrammatically in Fig. 7 (b). In Fig. 7 (c), we show the corresponding changes of the extremal surface inside the Penrose diagram. Starting from the extremal surface extending close to the singularity, the slice quickly deforms into the one further away from the singularity before the extremal surface ceases to exist. In this case, the generalized volume does not have a dual quantum complexity at late times.

## 6 Conclusion

In the Complexity=Anything conjecture, a much wider class of observables is considered as viable candidates for the dual of holographic complexity. The core of evaluating the generalized volume, which is the complexity dual, is to find the extremal slice defined by a scalar function. In this study, we explored the CAny conjecture in four- and five-dimensional Gauss-Bonnet gravity in anti-de Sitter space. Specifically, we demonstrated the universality of the existence of the complexity dual at late times in 4D. Notably, the smallest radius to which the extremal surface extends always approaches a constant value at late times. This guarantees the finite asymptotic value of the conserved momentum and thus a constant increasing rate of the volume-complexity at late times. We observed that starting from the boundary time  $\tau = 0$ , the conserved momentum grows monotonically and the minimal radius of the extremal surface decreases monotonically to their corresponding finite asymptotic values at the local maximum of the effective potential. In cases where multiple local maxima co-exist, depending on the shape of the effective potential, phase transitions of the extremal surface can emerge if the local maximum closer to the singularity has a larger peak value than the outermost one. Otherwise, the extremal slice follows a similar pattern as in the single-peak potential. Furthermore, we showed that dipping slice on which  $P_\nu$  decreases with time does not generate the largest generalized volume and can be ignored in the computation. We argued that this feature extends beyond the Gauss-Bonnet gravity and is solely determined by the shape of the effective potential of a specific model.

The Gauss-Bonnet gravity in 4D and higher dimensions are dramatically different; the 4D gravity has time-like singularities and higher-D models all exhibit space-like singularities. In the 5D case, we showed that the universality of extremal slices at late times observed in 4D is not present, and only models with certain finite range of coupling parameters can serve as viable duals to the complexity. For coupling parameters outside the range, one can nevertheless evaluate the generalized volume according to the proposed formula. However, we found that the extremal surface only exists for a finite boundary time in this scenario and cannot replicate the constant growing feature of the complexity at late times.

In summary, this note investigates the CAny proposal in the Gauss-Bonnet gravity and extends the discussion to include the phase transitions of the extremal slices as well as the deformations of the extremal slices in various scenarios in the Gauss-Bonnet gravity. This study may stimulate further quest to the understanding of the quantum nature of gravity and shed light to the interiors of the black holes.

## Acknowledgments

X.W would like to acknowledge the support of the start-up grant from the Wenzhou Institute of University of Chinese Academy of Sciences.



## References

- [1] A. Almheiri, T. Hartman, J. Maldacena, E. Shaghoulian, and A. Tajdini, *The entropy of Hawking radiation*, *Rev. Mod. Phys.* **93** (2021), no. 3 035002, [[arXiv:2006.06872](#)].
- [2] D. N. Page, *Average entropy of a subsystem*, *Phys. Rev. Lett.* **71** (1993) 1291–1294, [[gr-qc/9305007](#)].
- [3] D. N. Page, *Information in black hole radiation*, *Phys. Rev. Lett.* **71** (1993) 3743–3746, [[hep-th/9306083](#)].
- [4] T. Hartman and J. Maldacena, *Time Evolution of Entanglement Entropy from Black Hole Interiors*, *JHEP* **05** (2013) 014, [[arXiv:1303.1080](#)].
- [5] L. Susskind, *Computational Complexity and Black Hole Horizons*, *Fortsch. Phys.* **64** (2016) 24–43, [[arXiv:1403.5695](#)]. [Addendum: *Fortsch. Phys.* **64**, 44–48 (2016)].
- [6] D. Stanford and L. Susskind, *Complexity and Shock Wave Geometries*, *Phys. Rev. D* **90** (2014), no. 12 126007, [[arXiv:1406.2678](#)].
- [7] J. Couch, W. Fischler, and P. H. Nguyen, *Noether charge, black hole volume, and complexity*, *JHEP* **03** (2017) 119, [[arXiv:1610.02038](#)].
- [8] A. Belin, R. C. Myers, S.-M. Ruan, G. Sárosi, and A. J. Speranza, *Does Complexity Equal Anything?*, *Phys. Rev. Lett.* **128** (2022), no. 8 081602, [[arXiv:2111.02429](#)].
- [9] A. Belin, R. C. Myers, S.-M. Ruan, G. Sárosi, and A. J. Speranza, *Complexity equals anything II*, *JHEP* **01** (2023) 154, [[arXiv:2210.09647](#)].
- [10] M.-T. Wang, H.-Y. Jiang, and Y.-X. Liu, *Generalized Volume-Complexity for RN-AdS Black Hole*, [[arXiv:2304.05751](#)].
- [11] R.-Q. Yang, *Strong energy condition and complexity growth bound in holography*, *Phys. Rev. D* **95** (2017), no. 8 086017, [[arXiv:1610.05090](#)].
- [12] Y.-S. An, R.-G. Cai, and Y. Peng, *Time Dependence of Holographic Complexity in Gauss-Bonnet Gravity*, *Phys. Rev. D* **98** (2018), no. 10 106013, [[arXiv:1805.07775](#)].
- [13] A. Ghodsi, S. Qolibikloo, and S. Karimi, *Holographic complexity in general quadratic curvature theory of gravity*, *Eur. Phys. J. C* **80** (2020), no. 10 920, [[arXiv:2005.08989](#)].
- [14] T. Mandal, A. Mitra, and G. S. Punia, *Action complexity of charged black holes with higher derivative interactions*, *Phys. Rev. D* **106** (2022), no. 12 126017, [[arXiv:2205.11201](#)].
- [15] H. Babaei-Aghbolagh, D. M. Yekta, K. Velni Babaei, and H. Mohammadzadeh, *Complexity growth in Gubser–Rocha models with momentum relaxation*, *Eur. Phys. J. C* **82** (2022), no. 4 383, [[arXiv:2112.10725](#)].
- [16] R.-G. Cai, S. He, S.-J. Wang, and Y.-X. Zhang, *Revisit on holographic complexity in two-dimensional gravity*, *JHEP* **08** (2020) 102, [[arXiv:2001.11626](#)].
- [17] S. A. Hosseini Mansoori and M. M. Qaemmaqami, *Complexity growth, butterfly velocity and black hole thermodynamics*, *Annals Phys.* **419** (2020) 168244, [[arXiv:1711.09749](#)].
- [18] R. Auzzi, G. Nardelli, G. P. Ungureanu, and N. Zenoni, *Volume complexity of dS bubbles*, *Phys. Rev. D* **108** (2023), no. 2 026006, [[arXiv:2302.03584](#)].
- [19] R. Emparan, A. M. Frassino, M. Sasieta, and M. Tomašević, *Holographic complexity of quantum black holes*, *JHEP* **02** (2022) 204, [[arXiv:2112.04860](#)].

- [20] H. Zolfi, *Complexity and Multi-boundary Wormholes in  $2 + 1$  dimensions*, *JHEP* **04** (2023) 076, [[arXiv:2302.07522](#)].
- [21] Z.-Y. Fan and M. Guo, *Holographic complexity and thermodynamics of AdS black holes*, *Phys. Rev. D* **100** (2019) 026016, [[arXiv:1903.04127](#)].
- [22] J. Haferkamp, P. Faist, N. B. Kothakonda, J. Eisert, and N. Yunger Halpern, *Linear growth of quantum circuit complexity*, *Nature Physics* **18** (2022), no. 5 528–532.
- [23] J. Maldacena and L. Susskind, *Cool horizons for entangled black holes*, *Fortsch. Phys.* **61** (2013) 781–811, [[arXiv:1306.0533](#)].
- [24] A. R. Brown, D. A. Roberts, L. Susskind, B. Swingle, and Y. Zhao, *Complexity, action, and black holes*, *Phys. Rev. D* **93** (2016), no. 8 086006, [[arXiv:1512.04993](#)].
- [25] A. R. Brown, D. A. Roberts, L. Susskind, B. Swingle, and Y. Zhao, *Holographic Complexity Equals Bulk Action?*, *Phys. Rev. Lett.* **116** (2016), no. 19 191301, [[arXiv:1509.07876](#)].
- [26] A. Mounim and W. Mück, *Reparametrization dependence and holographic complexity of black holes*, *Phys. Rev. D* **105** (2022), no. 2 026024, [[arXiv:2106.01897](#)].
- [27] S. N. Sajadi and M. R. Setare, *Action-complexity in GMMG and EGMG*, *Gen. Rel. Grav.* **54** (2022), no. 12 157.
- [28] T. Anegawa, N. Iizuka, S. K. Sake, and N. Zenoni, *Is action complexity better for de Sitter space in Jackiw-Teitelboim gravity?*, *JHEP* **06** (2023) 213, [[arXiv:2303.05025](#)].
- [29] K. Meng, *Holographic complexity of Born-Infeld black holes*, *Eur. Phys. J. C* **79** (2019), no. 12 984, [[arXiv:1810.02208](#)].
- [30] E. Jørstad, R. C. Myers, and S.-M. Ruan, *Complexity=Anything: Singularity Probes*, [[arXiv:2304.05453](#)].
- [31] S. E. Aguilar-Gutierrez, M. P. Heller, and S. Van der Schueren, *Complexity = Anything Can Grow Forever in de Sitter*, [[arXiv:2305.11280](#)].
- [32] P. G. Fernandes, P. Carrilho, T. Clifton, and D. J. Mulryne, *The 4d einstein-gauss-bonnet theory of gravity: a review*, *Classical and Quantum Gravity* **39** (2022), no. 6 063001.
- [33] D. Glavan and C. Lin, *Einstein-gauss-bonnet gravity in four-dimensional spacetime*, *Physical review letters* **124** (2020), no. 8 081301.
- [34] P. G. S. Fernandes, P. Carrilho, T. Clifton, and D. J. Mulryne, *Derivation of Regularized Field Equations for the Einstein-Gauss-Bonnet Theory in Four Dimensions*, *Phys. Rev. D* **102** (2020), no. 2 024025, [[arXiv:2004.08362](#)].
- [35] N. Dadhich, *On causal structure of 4D-Einstein-Gauss-Bonnet black hole*, *Eur. Phys. J. C* **80** (2020), no. 9 832, [[arXiv:2005.05757](#)].
- [36] S.-W. Wei, Y.-X. Liu, and R. B. Mann, *Black Hole Solutions as Topological Thermodynamic Defects*, *Phys. Rev. Lett.* **129** (2022), no. 19 191101, [[arXiv:2208.01932](#)].
- [37] C. Liu and J. Wang, *Topological natures of the Gauss-Bonnet black hole in AdS space*, *Phys. Rev. D* **107** (2023), no. 6 064023, [[arXiv:2211.05524](#)].
- [38] R. Li, C. Liu, K. Zhang, and J. Wang, *Topology of the landscape and dominant kinetic path for the thermodynamic phase transition of the charged Gauss-Bonnet AdS black holes*, [[arXiv:2302.06201](#)].

- [39] R. Li and J. Wang, *Generalized free energy landscapes of the charged Gauss-Bonnet AdS black holes in diverse dimensions*, [arXiv:2304.03425](#).
- [40] R. Li and J. Wang, *Energy and entropy compensation, phase transition and kinetics of four dimensional charged Gauss-Bonnet Anti-de Sitter black holes on the underlying free energy landscape*, *Nucl. Phys. B* **976** (2022) 115714, [[arXiv:2012.05424](#)].
- [41] D. G. Boulware and S. Deser, *String Generated Gravity Models*, *Phys. Rev. Lett.* **55** (1985) 2656.
- [42] A. Buchel and R. C. Myers, *Causality of holographic hydrodynamics*, *Journal of High Energy Physics* **2009** (2009), no. 08 016.